Electronic Supplementary Material (ESI) for ChemComm.

Supporting Information for

Selective P_4 activation by an organometallic nickel(I) radical: Formation of a dinuclear nickel(II) tetraphosphide and related di- and trichalcogenides

*Stefan Pelties,[a] Dirk Herrmann,[a] Bas de Bruin,[b] František Hartl[c] and Robert Wolf[a,]**

[a] University of Regensburg, Institute of Inorganic Chemistry, 93040 Regensburg. [b] University of Amsterdam, Van 't Hoff Institute for Molecular Sciences, Science Park 904, 1098 XH Amsterdam, The Netherlands. [c] University of Reading, Department of Chemistry, Whiteknights, Reading, RG6 6AD, United Kingdom

The supporting information contains:

(S1) Synthesis and Characterization of 1–8

All experiments were performed under an atmosphere of dry argon using standard Schlenk techniques or a MBraun UniLab glovebox. Solvents were purified, dried, and degassed with an MBraun SPS800 solvent purification system. NMR spectra were recorded on Bruker Avance 300 and Avance 400 spectrometers at 300 K and internally referenced to residual solvent resonances.[1,2] Melting points were measured on samples in sealed capillaries on a Stuart SMP10 melting point apparatus. UV/Vis spectra were recorded on a Varian Cary 50 spectrophotometer. Elemental analyses were determined by the analytical department of Regensburg University. The starting materials [IMesH]Cl, [(C_5H_5)NiCl(IDipp)], [(C_5Me_5)NiCl(IDipp)] were prepared according to literature procedures.[3–5] Yellow sulfur, grey selenium, grey tellurium, TEMPO, and $LiBEt_3H$ (1M solution in THF) were purchased from Aldrich and used as received.

Synthesis of [(C_5H_5)NiCl(IMes)]: The preparation of [CpNiCl(IMes)] is based on a published synthesis of [CpNiCl(IDipp)].[4] Cp_2Ni (2.00 g, 10.6 mmol, 1.0 eq.) and [IMesH]Cl (3.79 g, 11.1 mmol) were dissolved in THF (100 mL). The suspension was refluxed for 16 h. A colour change to dark purple was observed in the first 30 min. The solvent was subsequently removed and the residue was extracted with toluene (ca. 100 mL). The resulting solution was concentrated to ca. 20 mL. Purple crystals of [CpNiCl(IMes)] formed upon standing at room temperature. These were isolated, washed with *n*-pentane (10 mL), and dried in vacuo. Yield: 2.99 g (61%); m.p.: >140 °C (slow decomp. to a black solid); UV/Vis (THF): λ_{max} (nm, ε_{max} /L·mol^{-1}·cm^{-1})): 321 (7300), 511 (400); elemental analysis calcd. for $C_{26}H_{29}ClN_2Ni$ (M = 465.7): C 67.06, H 6.71, N 6.02, found: C 67.36, H 6.22, N 5.91; ^1H NMR (d_8-THF, 300 K, 400.13 MHz): δ (ppm): 2.13 (s, 18H, CH_3), 4.71 (s, 5H, Cp), 6.19 (s, 2H, NC-H), 6.87 (s, 4H, *meta*-H_{Ar}); $^{13}C\{^1H\}$ NMR (d_8-THF, 300 K, 100.61 MHz): δ (ppm): 18.6 (CH_3), 21.1 (CH_3), 92.3 (Cp), 124.0 (N*C*-H), 129.4 (C_{Ar}), 137.3 (C_{Ar}), 139.0 (C_{Ar}), 168.8 (N*C*N).

Synthesis of [(C_5H_5)Ni(IDipp)] (1): KC_8 (467 mg, 3.46 mmol, 1.1 eq) was added in small portions to a cooled (−80 °C) solution of [CpNiCl(IDipp)] (1.722 g, 3.143 mmol, 1.0 eq) in THF (100 mL). After stirring the reaction mixture for three days at room temperature, the solvent was removed, and the dark residue was extracted with toluene (6×120 mL). The solvent was removed, and the yellow solid was dried in vacuo. Compound **1** was isolated as yellow powder in 86% yield. In some instances, the ^1H NMR spectrum showed small signals of unknown impurities, which were removed by recrystallization from toluene giving yellow crystals of **1** in 51% yield. M.p.: >95 °C (slow decomp. to a dark brown solid); UV/Vis (*n*-hexane): λ_{max} (nm, ε_{max} /L·mol^{-1}·cm^{-1})): 324 (8300), 402 (8100); effective magnetic moment (C_6D_6): μ_{eff} = 2.3(1) μ_B; elemental analysis calcd. for $C_{26}H_{29}N_2Ni$ (M = 428.2): C 75.01, H 8.07, N 5.47, found: C 75.02, H 7.94, N 5.43; ^1H NMR (C_6D_6, 300 K, 300.13 MHz): δ (ppm): −40.7 (br s, 5H, Cp), 1.3 (br s, 12H, CH(CH_3)$_2$), 2.0 (br s, 12H, CH(CH_3)$_2$), 3.5 (br s, 2H, *para*-H_{Ar}), 5.1 (br s, 4H, *meta*-H_{Ar}), 6.8 (br s, 4H, C*H*(CH_3)$_2$), 26.5 (br s, 2H, NC-H).

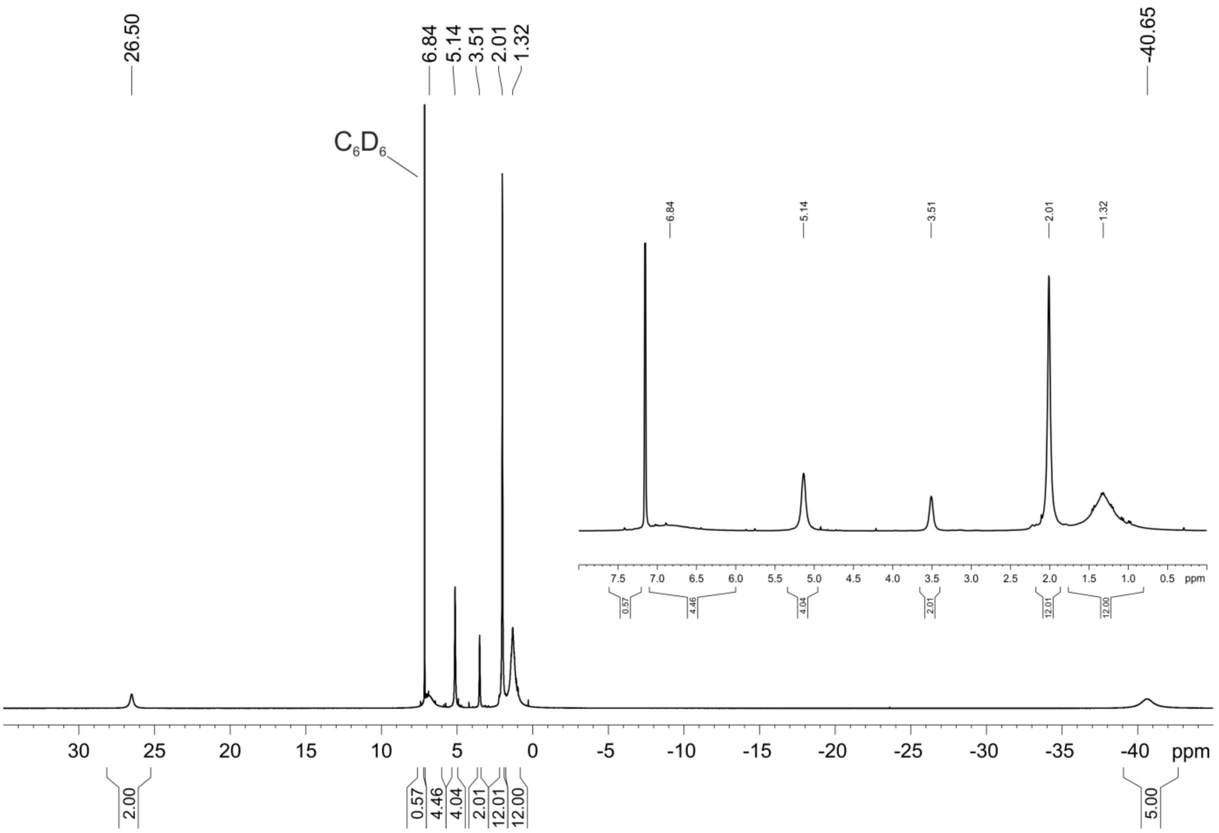

Figure S1. ^{1}H NMR spectrum of [CpNi(IDipp)] (**1**, 300.13 MHz, C_6D_6, 300 K).

Synthesis of [(C_5H_5)Ni(IMes)] (2): KC_8 (154.2 mg, 1.141 mmol, 1.05 eq) was added in small portions to a cooled (−80 °C) solution of [CpNiCl(IMes)] (503.7 g, 1.086 mmol, 1.0 eq) in THF (20 mL). The reaction mixture was stirred for 14 h at room temperature. The solvent was subsequently removed, and the dark residue was extracted with toluene (20 mL). The solution was concentrated to ca. 7 mL. Yellow crystals of **2** formed upon cooling this solution to −15 °C. Yield: 178 mg (38%); m.p.: >87 °C (slow decomp. to a brown solid); UV/Vis (THF): λ_{max} (nm, ε_{max} /L·mol^{-1}·cm^{-1})): 337 (5400), 400 (4900), 425 (5700); effective magnetic moment (C_6D_6): μ_{eff} = 2.3(1) μ_B; elemental analysis calcd. for $C_{26}H_{29}N_2Ni$ (M = 428.2): C 72.93, H 6.83, N 6.54, found: C 73.39, H , N 6.78, N 6.44; ^{1}H NMR (C_6D_6, 300 K, 400.13 MHz): δ (ppm): −38.2 (br s, 5H, Cp), 1.6 (br s, 6H, *para*-CH_3), 3.5 (br s, 12H, *ortho*-CH_3), 4.6 (br s, 4H, *meta*-H_{Ar}), 25.4 (br s, 2H, NC-H). Compound **2** contains a small amount (<5% according to the ^{1}H NMR analysis) of putative [CpNiH(IMes)], which could not be removed by recrystallisation (see Figure S2).

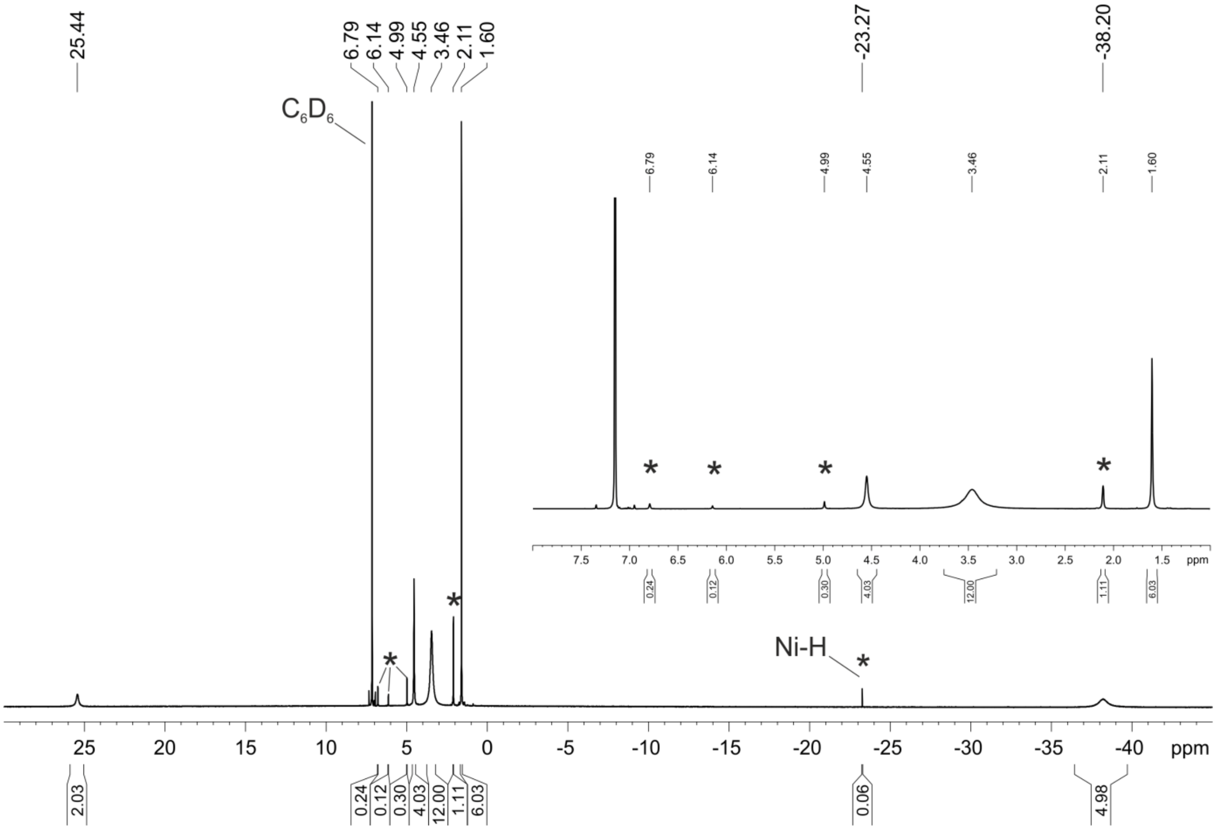

Figure S2. ^{1}H NMR spectrum of [CpNi(IMes)] (**2**, 400.13 MHz, C_6D_6, 300 K). The signals assigned to the by-product [CpNiH(IMes)] are labeled with an asterisk.

Synthesis of [(C_5Me_5)Ni(IDipp)] (3): KC_8 (115 mg, 0.853 mmol, 1.1 eq) was added in small portions to a cooled (−80 °C) solution of [Cp*NiCl(IDipp)] (479 g, 0.775 mmol, 1.0 eq) in THF (20 mL). The solvent was removed after stirring the reaction mixture for four days at room temperature, and the dark residue was extracted with toluene (10 mL and 5 mL). The solution was concentrated to ca. 3 mL. Yellow crystals of **3** formed upon cooling this solution to −35 °C Yield: 246 mg (55%); m.p.: >98 °C (slow decomp. to a black solid); UV/Vis (*n*-hexane): $\lambda_{\max}$ (nm, $\varepsilon_{\max}$ /L·mol^{-1}·cm^{-1})): sh351 (6600), 371 (7100), 476 (9400); effective magnetic moment (C_6D_6): $\mu_{\text{eff}} = 2.2(1)\ \mu_B$; elemental analysis calcd. for $C_{37}H_{51}N_2Ni$ (M = 582.5): C 76.29, H 8.83, N 4.81, found: C 76.56, H , N 8.67, N 4.69; ^{1}H NMR (C_6D_6, 300 K, 400.13 MHz): δ (ppm): 1.8 (br s, 12H, CH(CH_3)$_2$), 2.7−2.9 (br m, 16H, CH(CH_3)$_2$/*para*-H), 5.6 (br s, 4H, *meta*-H$_{\text{Ar}}$), 6.30 (br s, 4H, C*H*(CH$_3$)$_2$), 30.8 (br s, 2H, NC-H), 103.6 (br s, 15H, C_5Me_5).

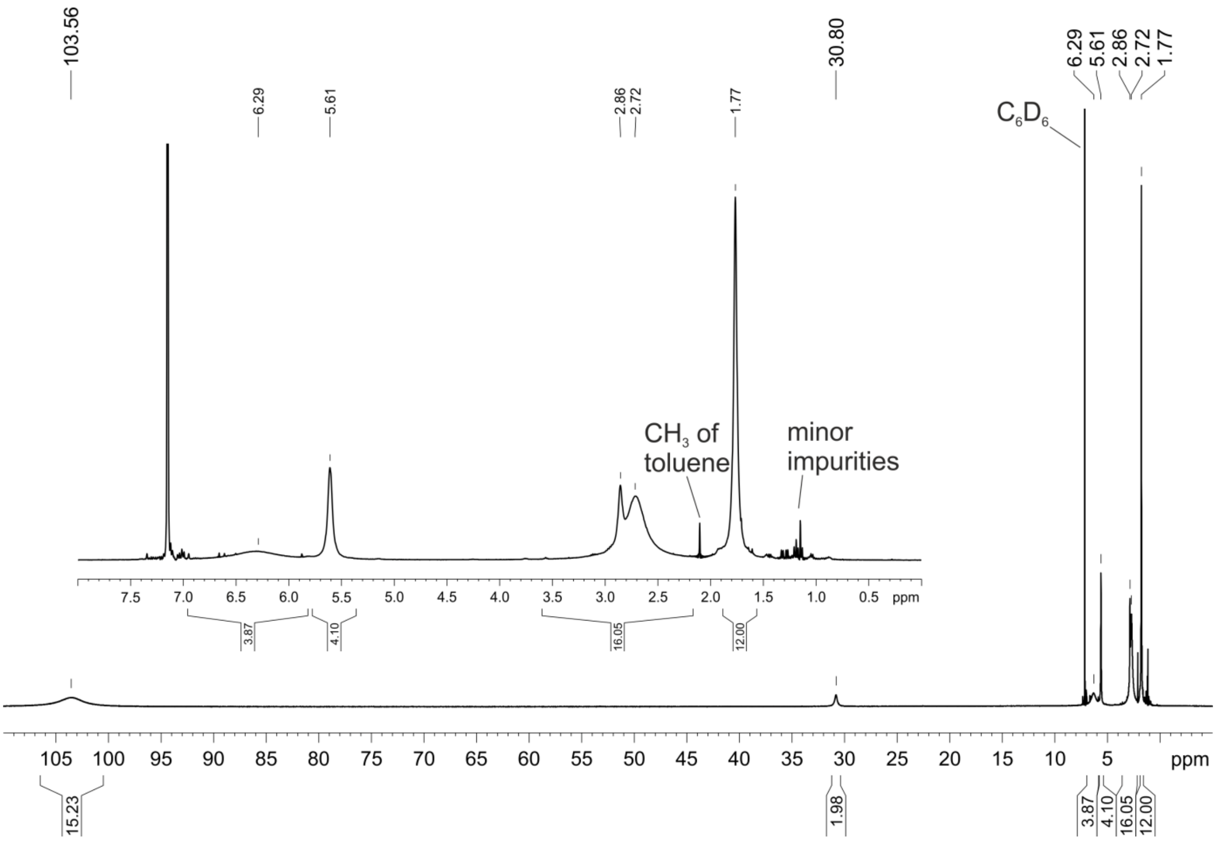

Figure S3. ^{1}H NMR spectrum of [(C_5Me_5)Ni(IDipp)] (**3**, 400.13 MHz, C_6D_6, 300 K).

Synthesis of [(C_5H_5)Ni(SPh)(IDipp)] (4): A solution of **1** (28.2 mg, 0.0550 mmol, 2.0 eq.) in THF (3 mL) was added to a solution of phenyl disulfide (6.0 mg, 0.027 mmol, 1.0 eq.) in THF (3 mL) at room temperature. The solvent was removed after stirring the reaction solution for 20 min, and the crude product was extracted with *n*-hexane. Dark brown crystals formed upon cooling the solution to −35 °C. Yield: 21 mg (62%); elemental analysis calcd. for $C_{38}H_{46}N_2NiS$ (M = 621.6): C 73.43, H 7.46, N 4.51, found: C 73.20, H 7.49, N 4.23; ^{1}H NMR ($CDCl_3$, 300 K, 400.13 MHz): δ (ppm): 1.08 (d, $^3J_{HH}$ = 6.9 Hz, 12H, CH(CH_3)$_2$), 1.39 (d, $^3J_{HH}$ = 6.9 Hz, 12H, CH(CH_3)$_2$), 2.90 (bs, 4H, CH(CH$_3$)$_2$), 4.56 (s, 5H, Cp), 6.64 (m, 3H, *meta-*/*para*-H$_{Ph}$), 6.86 (m, 2H, *ortho*-H$_{Ph}$), 7.09 (s, 2H, NC-H), 7.30 (d, $^3J_{HH}$ = 7.8 Hz, 4H, *meta*- H$_{Dipp}$), 7.46 (t, $^3J_{HH}$ = 7.8 Hz, 2H, *para*- H$_{Dipp}$); ^{13}C{^{1}H} NMR (ppm): 22.5, 26.2, 28.8, 92.1, 120.0, 123.9, 125.2, 126.2, 129.9, 137.1, 146.2, 148.2 174.4.

Synthesis of [(C_5H_5)Ni(TEMPO)(IDipp)] (5): A solution of TEMPO (19.4 mg, 0.124 mmol, 1.0 eq.) in toluene (2 mL) was added to a solution of **1** (63.6 mg, 0.124 mmol, 1.0 eq.) in toluene (2 mL) at room temperature. The reaction solution was slightly reduced in volume after stirring for 1 h. Dark pink X-ray quality crystals of **5** formed after cooling the solution to −35 °C. Yield: 68 mg (65%); m.p.: >70 °C (slow decomp. to a dark brown oil); UV/Vis (*n*-hexane): λ_{max} (nm, ε_{max} /L·mol^{-1}·cm^{-1})): 510 (593); elemental analysis calcd. for $C_{41}H_{59}N_3NiO$ (M = 668.6): C 73.65, H 8.89, N 6.28, found: C 73.69, H 8.77, N 6.34; ^{1}H NMR (C_6D_6, 300 K, 400.13 MHz): δ (ppm): 0.89 (s, 6H, CH$_3$-TEMPO), 0.96-1.28 (m, 4H, CH$_2$), 1.00 (d, $^3J_{HH}$ = 6.8 Hz, 12H, CH(CH_3)$_2$), 1.46-1.56 (m, 2H, CH$_2$), 1.46 (d,

$^{3}J_{HH}$ = 6.8 Hz, 12H, CH(C*H*$_3$)$_2$), 1.67 (s, 6H, CH$_3$-TEMPO), 3.12 (sept, $^{3}J_{HH}$ = 6.8 Hz, 4H, C*H*(CH$_3$)$_2$), 5.93 (s, 5H, Cp), 6.61 (s, 2H, NC-H), 7.24 (d, $^{3}J_{HH}$ = 7.5 Hz, 4H, *meta*-H$_{Ar}$), 7.32 (t, $^{3}J_{HH}$ = 7.7 Hz, 2H, *para*-H$_{Ar}$); ^{13}C{^{1}H} NMR (C_6D_6, 300 K, 100.61 MHz): δ (ppm): 16.9 (N-CH$_2$-*C*H$_2$), 22.6 (CH(*C*H$_3$)$_2$), 23.3 (CH$_3$-TEMPO), 26.5 (CH(*C*H$_3$)$_2$), 29.1 (*C*H(CH$_3$)$_2$), 31.9 (CH$_3$-TEMPO), 37.1 (N-*C*H$_2$-CH$_2$), 63.1 (ON*C*), 109.6 (Cp), 124.0 (*meta*-C), 125.5 (N*C*-H), 130.1 (p*ara*-C), 137.3 (*ipso*-C), 147.0 (*ortho*-C), 183.6 (N*C*N).

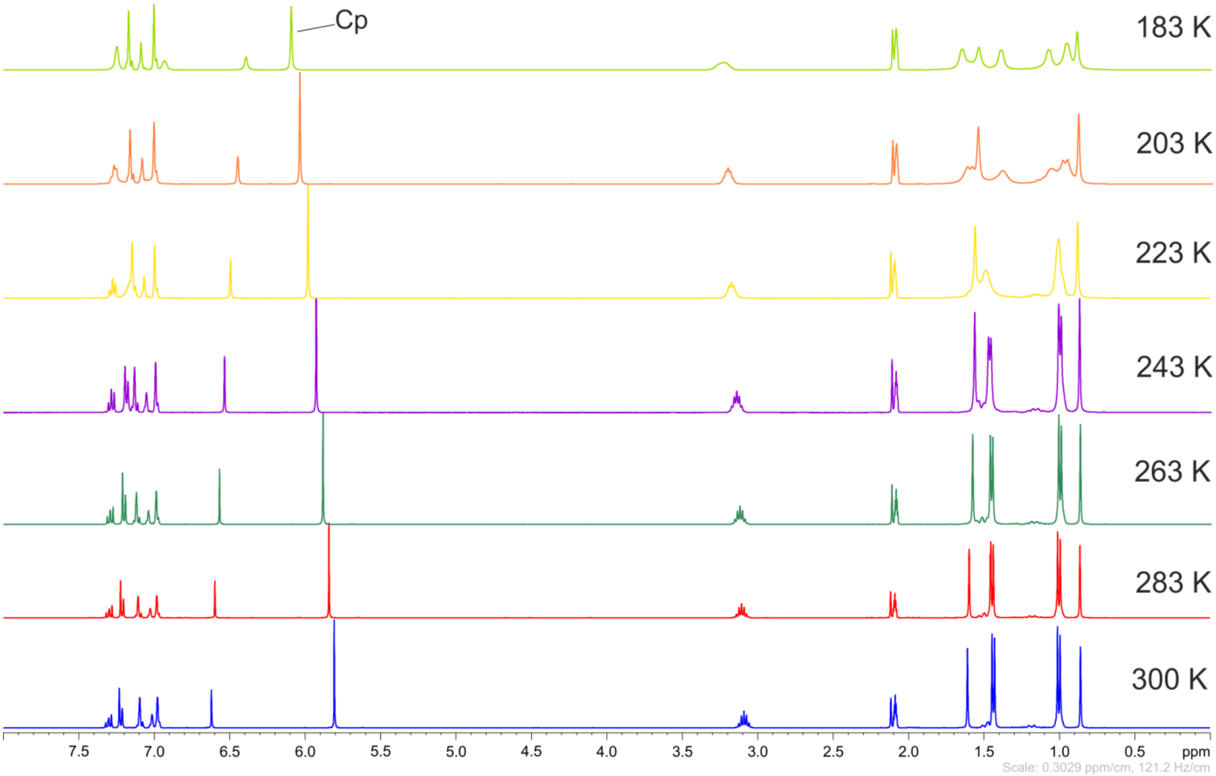

Figure S4. ^{1}H NMR spectrum of [(C$_5$H$_5$)Ni(TEMPO)(IDipp)] (**5**, 400.13 MHz, C_7D_8) at different temperatures.

Synthesis of [(C$_5$H$_5$)Ni(IDipp)$_2$(*μ*-η^1:η^1-S$_2$)] (6-S) and [(C$_5$H$_5$)Ni(IDipp)$_2$(*μ*-η^1:η^1-S$_3$)] (7-S): S_8 (6.7 mg, 0.026 mmol, 1.0 eq.) was added to a solution of **1** (107.1 mg, 0.209 mmol, 8.0 eq.) in THF (5 mL) at room temperature. The resulting dark green solution was stirred for 14 h, and the solvent was removed afterwards. Blue X-ray quality crystals of **6-S** were obtained by extracting the raw product with *n*-hexane and cooling the solution to −35 °C. Yield (**6-S**): 47 mg (42%). The solid residue of the *n*-hexane extract was washed with diethyl ether. **7-S** was obtained as a purple powder by extracting the residue with THF and removing of the solvent of this filtrate. Yield (**7-S**): 18 mg (15%). X-ray quality crystals were obtained by cooling a concentrated solution of **7-S** in toluene to −35 °C. Analytical data for **6-S**: m.p.: >195 °C (slow decomp. to a dark grey solid); UV/Vis (*n*-hexane): λ_{max} (nm, ε_{max} /L·mol^{-1}·cm^{-1})): 415 (5900), sh540 (4238), 635 (10046); elemental analysis calcd. for $C_{64}H_{82}N_4Ni_2S_2$ (M = 1088.9): C 70.59, H 7.59, N 5.15, found: C 70.57, H 7.44, N 4.95; ^{1}H NMR (C_6D_6, 300 K, 400.13 MHz): δ (ppm): 0.96 (d, $^{3}J_{HH}$ = 6.7 Hz, 24H, CH(C*H*$_3$)$_2$), 1.52 (d, $^{3}J_{HH}$ = 6.7 Hz, 24H, CH(CH_3)$_2$), 3.14 (bs, 8H, CH(CH$_3$)$_2$), 4.65 (s, 10H, Cp), 6.45 (s, 4H, NC-H), 7.17-7.26 (m, 12H, H$_{Ar}$); ^{13}C{^{1}H} NMR (C_6D_6, 300 K, 100.61 MHz): δ (ppm): 23.2 (CH(CH$_3$)$_2$), 26.0 (CH(CH$_3$)$_2$), 28.9 (CH(CH$_3$)$_2$), 94.1 (Cp), 124.1 (NC-H), 124.7 (*meta*-C), 130.0 (p*ara*-C), 137.8 (*ipso*-C), 146.2 (*ortho*-C), 181.3 (NCN). Analytical data for **7-S**: m.p.: >173 °C (slow decomp. to a dark solid); UV/Vis (THF): λ_{max} (nm, ε_{max} /L·mol^{-1}·cm^{-1})): 370 (6000), 531 (8455); elemental analysis calcd. for $C_{64}H_{82}N_4Ni_2S_3\cdot C_4H_8O$ (M = 1121.0): C 68.46, H 7.60, N 4.70, found: C 68.04, H 7.14, N 4.67; ^{1}H NMR (d_8-THF, 300 K, 400.13 MHz): δ (ppm): 0.94 (d, $^3J_{HH}$ = 6.7 Hz, 24H, CH(CH_3)$_2$), 1.47 (d, $^3J_{HH}$ = 6.7 Hz, 24H, CH(CH_3)$_2$), 3.06 (bs, 8H, CH(CH$_3$)$_2$), 5.21 (s, 10H, Cp), 6.50 (s, 4H, NC-H), 7.19-7.33 (m, 12H, H$_{Ar}$); ^{13}C{^{1}H} NMR (d_8-THF, 300 K, 100.61 MHz): δ (ppm): 23.0 (CH(CH$_3$)$_2$), 26.1 (CH(CH$_3$)$_2$), 29.3 (CH(CH$_3$)$_2$), 92.2 (Cp), 124.3 (NC-H), 126.2 (*meta*-C), 130.1 (p*ara*-C), 138.3 (*ipso*-C), 147.1 (*ortho*-C), 178.6 (NCN).

Synthesis of [(C_5H_5)Ni(IDipp)$_2$(μ-η^1:η^1-Se$_2$)] (6-Se): Grey selenium (28.1 mg, 0.357 mmol, 1.0 eq.) was added to a solution of **1** (183.0 mg, 0.357 mmol, 1.0 eq.) in THF (5 mL) at room temperature. The resulting dark green solution was stirred for 16 h, and the solvent was removed afterwards. The residue was extracted with toluene, and the solution was layered with *n*-hexane to afford X-ray quality crystals of **6-Se** at room temperature overnight. The ^{1}H NMR spectrum of these crystals shows the presence of compound **7-Se** (ca. 10%) which was characterised by X-ray crystallography. Yield: 30 mg (31%); m.p.: >173 °C (decomp. to a black oil); UV/Vis (THF): λ_{max} (nm, ε_{max} /L·mol^{-1}·cm^{-1})): 435 (6000), 650 (5500); elemental analysis calcd. for $C_{64}H_{82}N_4Ni_2Se_2\cdot 0.5(C_6H_{14})$ (M = 1225.8): C 65.65, H 7.32, N 4.57, found: C 66.05, H 7.33, N 4.49; ^{1}H NMR (C_6D_6, 300 K, 400.13 MHz): δ (ppm): 0.95 (d, $^3J_{HH}$ = 6.7 Hz, 24H, CH(CH_3)$_2$, **6-Se**), 1.14 (d, $^3J_{HH}$ = 6.9 Hz, 2.4H, CH(CH_3)$_2$, **7-Se**), 1.48 (d, $^3J_{HH}$ = 6.9 Hz, 2.4H, CH(CH_3)$_2$, **7-Se**), 1.52 (d, $^3J_{HH}$ = 6.7 Hz, 24H, CH(CH_3)$_2$, **6-Se**), 2.87 (sept., 0.8H, $^3J_{HH}$ = 6.9 Hz, CH(CH$_3$)$_2$, **7-Se**), 3.11 (br s, 8H, CH(CH$_3$)$_2$, **6-Se**), 4.65 (s, 10H, Cp, **6-Se**), 5.18 (s, 1H, Cp, **7-Se**), 6.30 (s, 0.4H, NC-H, **7-Se**), 6.51 (s, 4H, NC-H, **6-Se**), 7.12−7.27 (m, 13H, H$_{Ar}$, 6-Se/7-Se); ^{13}C{^{1}H} NMR (C_6D_6, 300 K, 100.61 MHz): δ (ppm): 23.1 (CH(CH$_3$)$_2$), 26.2 (CH(CH$_3$)$_2$), 29.0 (CH(CH$_3$)$_2$), 94.4 (Cp), 124.0 (NC-H), 124.9 (*meta*-C), 130.0 (p*ara*-C), 137.8 (*ipso*-C), 146.4 (*ortho*-C), 182.4 (NCN).

Synthesis of [(C_5H_5)Ni(IDipp)$_2$(μ-η^1:η^1-Te$_2$)] (6-Te) Grey tellurium (18.1 mg, 0.142 mmol, 1.0 eq.) was added to a solution of **1** (72.7 mg, 0.142 mmol, 1.0 eq.) in THF (5 mL) at room temperature. The suspension was stirred for 7 days. A slow colour change from dark yellow to dark brown was observed. The solvent was removed, and the dark residue was extracted with diethyl ether. Cooling to −35 °C gave dark brown crystals of **6-Te**. Yield: 30 mg (31%) X-ray quality crystals were grown from a concentrated solution of **6-Te** in *n*-hexane at room temperature. M.p.: >165 °C (slow decomp. to a grey solid); UV/Vis (THF): λ_{max} (nm, ε_{max} /L·mol^{-1}·cm^{-1})): 308 (27800), 460 (6670), 521 (5670), 669 (5170); elemental analysis calcd. for $C_{64}H_{82}N_2Ni_2S_2\cdot 0.5(C_4H_{10}O)$ (M = 1317.0): C 60.19, H 6.66, N 4.25, found: C 60.31, H 6.54, N 4.27; ^{1}H NMR (C_6D_6, 300 K, 400.13 MHz): δ (ppm): 0.93 (d, $^3J_{HH}$ =

6.7 Hz, 24H, CH(CH_3)$_2$), 1.51 (d, $^3J_{\mathrm{HH}}$ = 6.7 Hz, 24H, CH(CH_3)$_2$), 3.15 (bs, 8H, C*H*(CH$_3$)$_2$), 4.70 (s, 10H, Cp), 6.45 (s, 4H, NC-H), 7.16 (m, 4H, *ortho*-H$_{\mathrm{Ar}}$), 7.22 (m, 8H, *meta*- H$_{\mathrm{Ar}}$); ^{13}C{^{1}H} NMR (C_6D_6, 300 K, 100.61 MHz): δ (ppm): 23.5 (CH(*C*H$_3$)$_2$), 26.2 (CH(*C*H$_3$)$_2$), 29.2 (*C*H(CH$_3$)$_2$), 94.9 (Cp), 124.1 (N*C*-H), 125.2 (*meta*-C), 130.0 (p*ara*-C), 138.0 (*ipso*-C), 146.4 (*ortho*-C), 186.3 (N*C*N).

Synthesis of [(C_5H_5)Ni(IDipp)$_2$(μ-η^1:η^1-P_4)] (8): P_4 (79.4 mg, 0.641 mmol, 1.0 eq.) was added to a solution of **1** (656.7 mg, 1.28 mmol, 2.0 eq.) in THF (20 mL) at room temperature. The resulting dark red solution was stirred for 2 h. Afterward, the solvent was removed completely. Compound **8** remained as an analytically pure, red powder. Yield: 727 mg (99%). Dark purple X-ray quality crystals formed by diffusing *n*-hexane into a concentrated THF solution of **8**. M.p.: >160 °C (slow decomp. to a black and colourless solid); UV/Vis (THF): $\lambda_{\max}$ (nm, $\varepsilon_{\max}$ /L·mol^{-1}·cm^{-1})): 395 (23700), 420 (10700), 508 (10700); elemental analysis calcd. for $C_{64}H_{82}N_4Ni_2P_4$ (M = 1148.7): C 66.92, H 7.20, N 4.88, found: C 66.85, H 7.23, N 4.61; ^{1}H NMR (d$_8$-THF, 300 K, 400.13 MHz): δ (ppm): 1.06 (d, $^3J_{\mathrm{HH}}$ = 6.8 Hz, 24H, CH(CH_3)$_2$), 1.43 (d, $^3J_{\mathrm{HH}}$ = 6.8 Hz, 24H, CH(CH_3)$_2$), 3.03 (bs, 8H, C*H*(CH$_3$)$_2$), 4.29 (s, 10H, Cp), 7.29 (s, 4H, NC-H), 7.36 (d, $^3J_{\mathrm{HH}}$ = 7.8 Hz, 8H, *meta*-H$_{\mathrm{Ar}}$), 7.49 (t, $^3J_{\mathrm{HH}}$ = 7.8 Hz, 4H, *para*-H$_{\mathrm{Ar}}$); ^{13}C{^{1}H} NMR (d$_8$-THF, 300 K, 100.61 MHz): δ (ppm): 23.6 (CH(*C*H$_3$)$_2$), 26.2 (CH(*C*H$_3$)$_2$), 29.4 (*C*H(CH$_3$)$_2$), 91.0 (Cp), 124.4 (*meta*-C), 125.7 (N*C*-H), 130.2 (p*ara*-C), 138.4 (*ipso*-C), 147.0 (*ortho*-C), 185.6 (N*C*N); ^{31}P{^{1}H} NMR: (d$_8$-THF, 300 K, 121.49 MHz): δ (ppm): −307.4 (t, $^1J_{\mathrm{PP}}$ = −190.5 Hz, 2P), −45.8 (t, $^1J_{\mathrm{PP}}$ = −190.5 Hz, 2P).

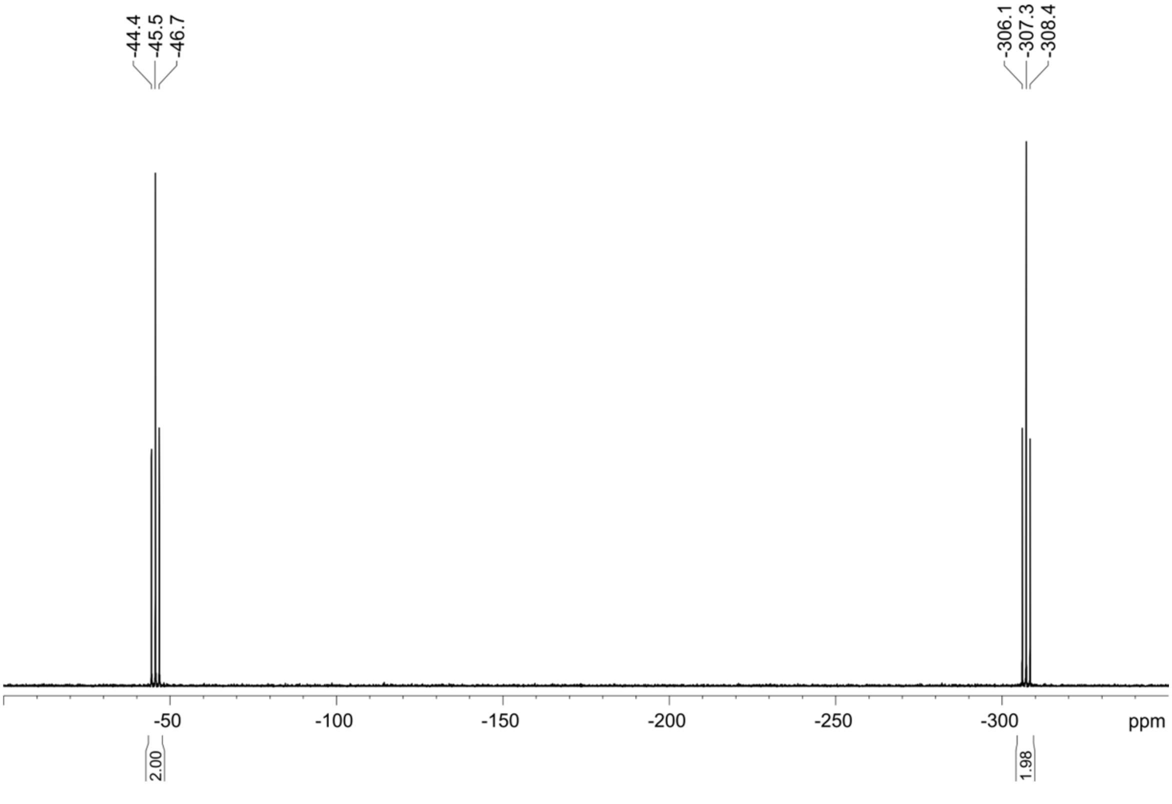

Figure S5. ^{31}P{^{1}H} NMR spectrum of the reaction solution of [CpNi(IDipp)(μ-µ^1:µ^1-P_4)] (**8**, 121.49 MHz, C_6D_6, 300 K).

Synthesis of (1-H): A 1M solution of $LiBEt_3H$ (0.50 mL, 0.50 mmol, 1.0 eq.) was added to a solution of [CpNiCl(IDipp)] (274 mg, 0.500 mmol, 1.0 eq.) in THF (10 mL) dropwise at 0 °C. The solution was allowed to warm up to room temperature, and was stirred for 14 h. The solvent of the resulting red solution was removed and extracted with 20 mL *n*-hexane. X-ray quality, red crystals of **1-H** formed upon cooling the solution to −15 °C. Yield: 98 mg (38%); m.p.: >185 °C (slow decomp. to a dark green solid); UV/Vis (*n*-hexane): λ_{max} (nm, ε_{max} /L·mol^{-1}·cm^{-1})): 365 (4500), 429 (710), 510 (150); elemental analysis calcd. for $C_{32}H_{42}N_2Ni$ (M = 513.4): C 74.86, H 8.25, N 5.46, found: C 74.65, H 8.20, N 5.35; ^{1}H NMR (C_6D_6, 300 K, 400.13 MHz): δ (ppm): −23.64 (s,1H, Ni-H),1.07 (d, $^3J_{HH}$ = 6.8 Hz, 12H, CH(C*H*$_3$)$_2$), 1.45 (d, $^3J_{HH}$ = 6.8 Hz, 12H, CH(C*H*$_3$)$_2$), 2.92 (sept, $^3J_{HH}$ = 6.8 Hz, 4H, C*H*(CH$_3$)$_2$), 4.91 (s, 5H, Cp), 6.45 (s, 2H, NC-H), 7.14 (d, $^3J_{HH}$ = 7.7 Hz, 4H, *meta*- H$_{Ar}$), 7.24 (t, $^3J_{HH}$ = 7.7 Hz, 2H, *para*- H$_{Ar}$); ^{13}C{^{1}H} NMR (C_6D_6, 300 K, 100.61 MHz): δ (ppm): 23.1 (CH(*C*H$_3$)$_2$), 24.9 (CH(*C*H$_3$)$_2$), 28.9 (*C*H(CH$_3$)$_2$), 86.9 (Cp), 122.5 (N*C*-H), 124.0 (*meta*-C), 129.7 (p*ara*-C), 138.7 (*ipso*-C), 146.2 (*ortho*-C), 188.6 (N*C*N).

Synthesis of (1-THF): **[**Cp_2Fe]PF_6 (10.8 mg, 0.0326 mmol, 1.0 eq.) was added to a solution of **1** (16.7 mg, 0.0326 mmol, 1.0 eq.) in THF (3 mL) at room temperature. The suspension was stirred for 14 h, and the solvent was removed afterwards. The residue was washed with *n*-hexane (ca. 3 mL) and extracted with THF (1.5 mL). Dark pink X-ray quality crystals of **1-THF** formed upon diffusing *n*-hexane into the THF solution. The ^{1}H NMR spectrum of these crystals shows the presence of an unidentified by-product (ca. 10%). Yield: 10 mg (42%). M.p.: >120 °C (decomp. to a brown solid); UV/Vis (THF): λ_{max} (nm, ε_{max} /L·mol^{-1}·cm^{-1})): 516 (467); elemental analysis calcd. for $C_{36}H_{49}N_2F_6NiOP$ (M = 729.46): C 59.28, H 6.77, N 3.84, found: C 58.84, H 6.52, N 3.79; ^{1}H NMR (d$_8$-THF, 300 K, 400.13 MHz): δ (ppm): 1.20 (d, $^3J_{HH}$ = 6.6 Hz, 12H, CH(C*H*$_3$)$_2$, 1-THF), 1.24 (d, $^3J_{HH}$ = 6.7 Hz, 1.2H, CH(C*H*$_3$)$_2$, by-product), 1.32 (d, $^3J_{HH}$ = 6.7 Hz, 1.2H, CH(C*H*$_3$)$_2$, by-product), 1.50 (d, $^3J_{HH}$ = 6.6 Hz, 12H, CH(C*H*$_3$)$_2$, 1-THF), 1.80 (m, 4H, THF), 2.54 (m, 0.4H, C*H*(CH$_3$)$_2$, by-product), 3.13 (m, 4H, C*H*(CH$_3$)$_2$, 1-THF), 4.60 (s, 5H, Cp, 1-THF), 7.46 – 7.64 (m, 0.3H, H$_{Ar}$, by-product), 7.48−7.67 (m, 6H, H$_{Ar}$, 1-THF), 7.73 (s, 2H, NC-H, 1-THF) 8.17 (s, 0.2H, NC-H, by-product) 9.44 (s, 0.1H, NCHN, by-product); ^{13}C{^{1}H} NMR (C_6D_6, 300 K, 100.61 MHz): δ (ppm): 22.5 (CH(*C*H$_3$)$_2$), 29.8 (*C*H(CH$_3$)$_2$), 94.9 (Cp), 125.4 (N*C*-H), 129.1 (*meta*-C), 131.5 (p*ara*-C), 132.8 (*ipso*-C), 146.2 (*ortho*-C); ^{19}F NMR (d$_8$-THF, 300 K, 100.61 MHz): δ (ppm): 72.8 (d, $^1J_{FP}$ = 710 Hz, 6F, PF$_6$). ^{31}P{^{1}H} NMR: (d$_8$-THF, 300 K, 121.49 MHz): δ (ppm) = -141.6 (sept., $^1J_{FP}$ = 710 Hz, 1P, PF$_6$).

(S2) X-ray crystallography

The single crystal X-ray diffraction data were recorded on an Agilent Technologies SuperNova diffractometer or, in case of compounds **2** and **3**, with an Agilent Technologies Gemini Ultra R with Cu K_{α} radiation (λ = 1.54178 Å). The data for **1-H** were recorded with an Agilent Technologies SuperMova diffractometer with Mo K_{α} radiation (λ = 0.71073 Å). Either semi-empirical multi-scan absorption corrections[6] or analytical ones[7] were applied to the data. The structures were solved with SHELXS[8] or SIR[9] and least-square refinements on F^2 were carried out with SHELXL.[7]
CCDC 995931-995941 contain the supplementary crystallographic data for this paper. These data can be obtained free of charge from The Cambridge Crystallographic Data Centre via www.ccdc.cam.ac.uk/data_request/cif.

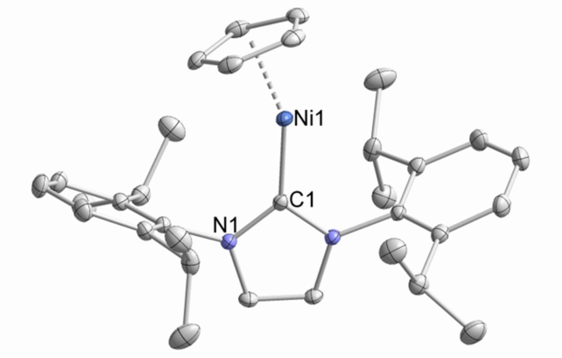

Figure S6. Solid-state molecular structure of **1**. The hydrogen atoms are omitted for clarity. Thermal ellipsoids are drawn at 40% level. Selected bond lengths [Å] and angles [°]: Ni1-C1 1.877(1), $(C_5H_5)_{centroid}$-Ni1 1.79(1), C1-Ni1-$(C_5H_5)_{centroid}$ 154.3(1).

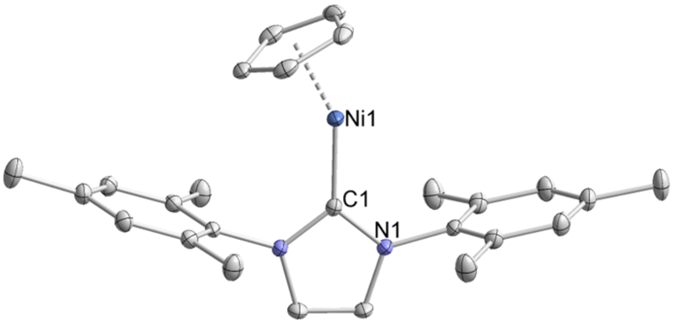

Figure S7. Solid-state molecular structure of **2**. The hydrogen atoms are omitted for clarity. Thermal ellipsoids are drawn at 40% level. Selected bond lengths [Å] and angles [°]: Ni1-C1 1.876(2), $(C_5H_5)_{centroid}$-Ni1 1.80(1), C1-Ni1-$(C_5H_5)_{centroid}$ 152.0(1).

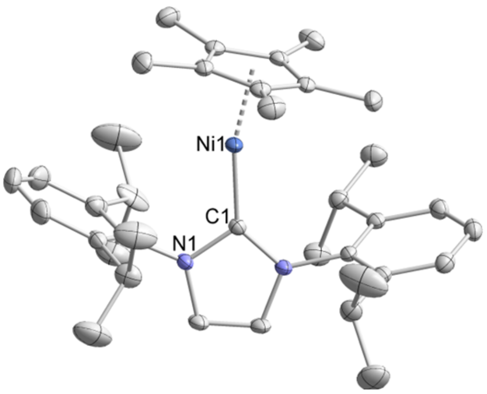

Figure S8. Solid-state molecular structure of **3**. The hydrogen atoms are omitted for clarity. Thermal ellipsoids are drawn at 40% level. Selected bond lengths [Å] and angles [°]: Ni1-C1 1.880(1), $(C_5H_5)_{centroid}$-Ni1 1.79(1), C1-Ni1-$(C_5H_5)_{centroid}$ 164.8(1).

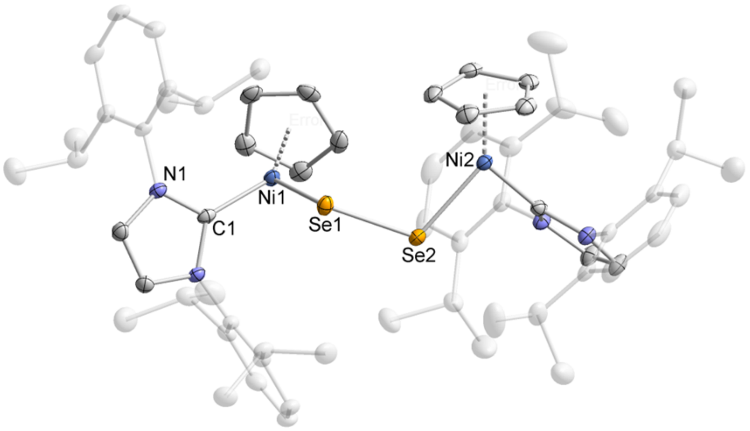

Figure S9. Solid-state molecular structure of **6-Se**. The hydrogen atoms are omitted for clarity. Thermal ellipsoids are drawn at 40% level. Selected bond lengths [Å] and angles [°]: Ni1-Se1/Ni2-Se2 2.3013(4)/2.2998(4), Se1-Se2 2.3361(3), Ni1-Se1-Se2 109.039(1), Ni1-Se1-Se2-Ni2 91.174(1).

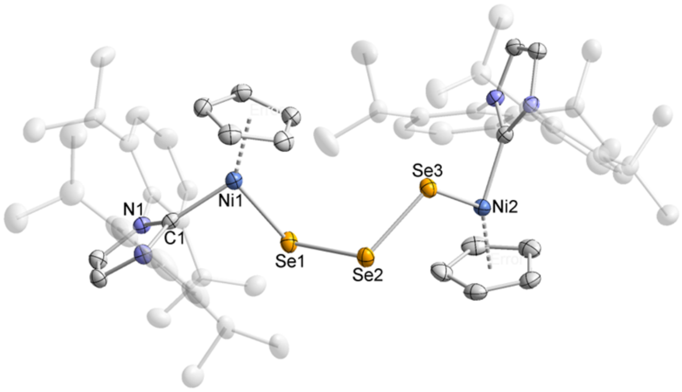

Figure S10. Solid-state molecular structure of **7-Se**. The hydrogen atoms are omitted for clarity. Thermal ellipsoids are drawn at 40% level. Selected bond lengths [Å] and angles [°]; the analogous bond distances and angles of a second crystallographically independent molecule in the asymmetric unit are given in parentheses: Ni1-Se1/Ni2-Se3 2.3068(6)/2.2838(6) (2.2847(6)/2.3341(5)), Se1-Se2/Se2-Se3 2.3335(4)/2.3318(5) (2.3282(5)/2.3341(5)), Ni1-Se1-Se2 108.480(2) (110.150(2)), Se1-Se2-Se3 109.117(2) (108.352(2)).

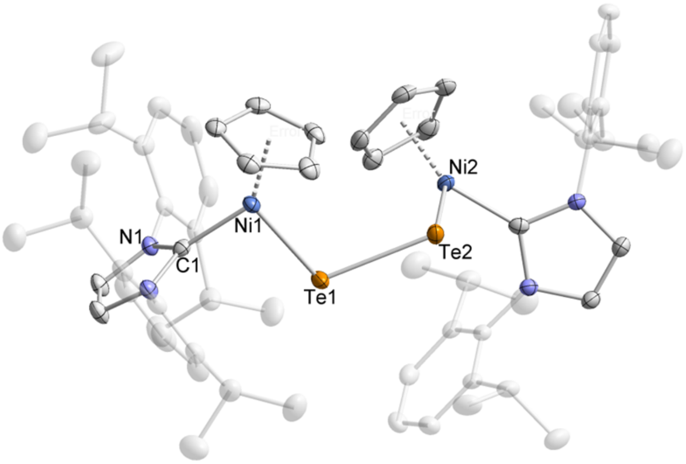

Figure S11. Solid-state molecular structure of **6-Te**. The hydrogen atoms are omitted for clarity. Thermal ellipsoids are drawn at 40% level. Selected bond lengths [Å] and angles [°]: Ni1-Te1/Ni2-Te2 2.4769(4)/2.4741(4), Te1-Te2 2.7063(2), Ni1-Te1-Te2 108.928(1), Ni1-Se1-Se2-Ni2 93.951(1).

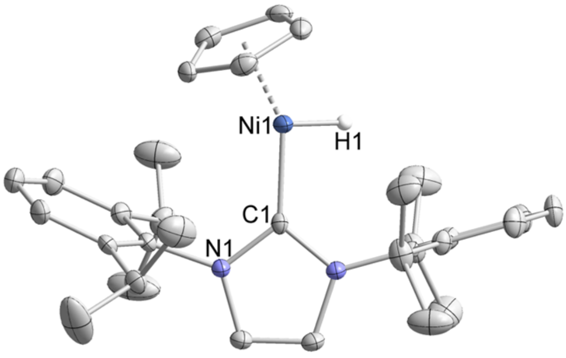

Figure S12. Solid-state molecular structure of **1-H**. Except for H1 the hydrogen atoms are omitted for clarity. Thermal ellipsoids are drawn at 40% level. Selected bond lengths [Å] and angles [°] the analogous bond distances and angles of the second molecule in the asymmetric unit are pointed out in brackets: Ni1-C1 1.849(4) (1.838(4)), $(C_5H_5)_{centroid}$-Ni1 1.77(1) (1.75(1)), C1-Ni1-$(C_5H_5)_{centroid}$ 148.3(1) (145.9(1)).

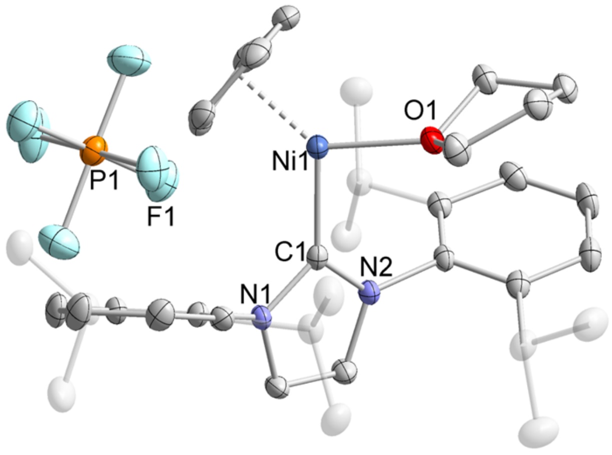

Figure S13. Solid-state molecular structure of **1-THF**. The hydrogen atoms are omitted for clarity. Thermal ellipsoids are drawn at 40% level. Selected bond lengths [Å] and angles [°]: Ni1-C1 1.903(2), $(C_5H_5)_{centroid}$-Ni1 1.77(1), C1-Ni1-$(C_5H_5)_{centroid}$ 131.3(1).

Table S1. Crystallographic data of 1, 2, 3, 5, 6-S, 7-S, 6-Se, 7-Se, 6-Te, 8, 1-H

	1	**2**	**3**	**5**
Empirical formula	$C_{32}H_{41}N_2Ni$	$C_{26}H_{29}N_2Ni$	$C_{37}H_{51}N_2Ni$	$C_{55}H_{75}N_3ONi$
Formula weight	512.38	428.22	582.50	852.89
Temperature/K	123.0(2)	123.1(2)	123.1(2)	123.0(2)
Crystal system	triclinic	orthorhombic	monoclinic	triclinic
Space group	P-1	*Pnma*	$P2_1/n$	P-1
a/Å	9.1771(3)	22.89090(10)	9.23970(10)	11.1354(8)
b/Å	9.3242(3)	11.10740(10)	18.6957(2)	12.2243(5)
c/Å	18.2253(5)	9.03710(10)	21.5074(2)	17.8241(7)
α/°	92.783(2)	90	90	87.524(4)
β/°	90.158(2)	90	93.7790(10)	85.065(5)
γ/°	116.159(3)	90	90	87.053(5)
Volume/Å^3	1397.63(7)	2297.76(3)	3707.17(7)	2412.2(2)
Z	2	4	4	2
ρ_{calc}mg/mm^3	1.218	1.238	1.044	1.174
m/mm^{-1}	1.146	1.299	0.913	0.877
F(000)	550.0	908.0	1260.0	924.0
Crystal size/mm^3	0.4 × 0.2 × 0.1	0.1 × 0.1 × 0.05	0.1 × 0.1 × 0.05	0.3 × 0.15 × 0.1
2Θ range for data collection	9.72 to 153.36°	7.724 to 134.068°	8.24 to 134.012°	7.246 to 147.526°
Index ranges	$-8 \leq h \leq 11, -11 \leq k \leq 11, -22 \leq l \leq 22$	$-27 \leq h \leq 27, -13 \leq k \leq 13, -10 \leq l \leq 10$	$-11 \leq h \leq 10, -22 \leq k \leq 22, -21 \leq l \leq 25$	$-13 \leq h \leq 13, -15 \leq k \leq 15, -22 \leq l \leq 19$
Reflections collected	14839	49162	19260	21977
Independent reflections	5715[R(int) = 0.0186]	2165 [R_{int} = 0.0377]	6556 [R_{int} = 0.0278]	9329 [R_{int} = 0.0504]
Data/restraints/parameters	5715/0/325	2165/2/167	6556/6/410	9329/0/561
Goodness-of-fit on F^2	1.035	1.120	1.074	1.041
R_1 ,wR_2 [I>=2σ (I)]	0.0293, 0.0737	0.0298, 0.0789	0.0384, 0.1080	0.0476, 0.1224
R_1 ,wR_2 [all data]	0.0304, 0.0745	0.0309, 0.0798	0.0427, 0.1121	0.0606, 0.1354

Largest diff. peak/ hole / e Å^{-3}	0.30/-0.30	0.21/-0.42	0.57/-0.43	0.65/-0.35
CCDC-	995938	995940	995941	995931

	6-S	**7-S**	**6-Se**
Empirical formula	$C_{64}H_{82}N_4Ni_2S_2$	$C_{128}H_{164}N_8Ni_4S_6$	$C_{70}H_{96}N_4Ni_2Se_2$
Formula weight	1088.88	2241.87	1268.84
Temperature/K	123.0(2)	123.0(2)	123.0(2)
Crystal system	triclinic	Monoclinic	monoclinic
Space group	P-1	*P*2$_1$/*n*	*P*2$_1$/*c*
a/Å	13.0231(5)	16.6760(4)	19.5580(3)
b/Å	14.2423(6)	18.4118(5)	20.1611(2)
c/Å	18.1147(5)	38.8467(10)	16.7962(2)
α/°	100.585(3)	90.00	90
β/°	95.676(3)	96.027(2)	96.1920(10)
γ/°	114.757(4)	90.00	90
Volume/Å^3	2940.41(19)	11861.4(5)	6584.28(14)
Z	2	4	4
ρ_{calc}mg/mm^3	1.230	1.255	1.280
m/mm^{-1}	1.766	2.086	2.282
F(000)	1164.0	4784.0	2672.0
Crystal size/mm^3	0.3 × 0.2 × 0.1	0.09 × 0.08 × 0.07	0.3 × 0.25 × 0.25
2Θ range for data collection	7.06 to 147.32°	6.64 to 147.52°	6.316 to 146.962°
Index ranges	-13 ≤ h ≤ 16, -17 ≤ k ≤ 17, -22 ≤ l ≤ 21	-20 ≤ h ≤ 18, -22 ≤ k ≤ 15, -47 ≤ l ≤ 47	-23 ≤ h ≤ 20, -24 ≤ k ≤
Reflections collected	21454	47574	32467
Independent reflections	11356[R(int) = 0.0211]	22844[R(int) = 0.0291]	12810[R(int) = 0.0254]
Data/restraints/parameters	11356/0/649	22844/0/1315	12810/0/703
Goodness-of-fit on F^2	1.024	1.010	1.022
R$_1$,wR$_2$ [I>=2σ (I)]	0.0302, 0.0738	0.0367, 0.0903	0.0296, 0.0709
R$_1$,wR$_2$ [all data]	0.0368, 0.0782	0.0475, 0.0961	0.0382, 0.0759
Largest diff. peak/ hole / e Å^{-3}	0.28/-0.32	0.72/-0.42	0.38/-0.58
CCDC-	995932	995935	995933

	7-Se	**6-Te**	**8**	**1-H**
Empirical formula	$C_{64}H_{82}N_4Ni_2Se_3$	$C_{70}H_{96}N_4Ni_2Te_2$	$C_{66}H_{86}N_4Ni_2O_{0.5}P_4$	$C_{32}H_{42}N_2Ni$
Formula weight	1261.63	1366.12	1184.69	513.39
Temperature/K	123.0(2)	123.0(2)	123.0(2)	123.0(2)
Crystal system	monoclinic	monoclinic	monoclinic	monoclinic
Space group	*P*2$_1$/*n*	*P*2$_1$/*c*	*P*2$_1$/*c*	*P*2$_1$/*n*
a/Å	16.8208(6)	19.69630(10)	13.7371(2)	12.4764(4)
b/Å	18.4669(10)	20.47330(10)	23.6940(5)	36.2568(10)
c/Å	39.0547(10)	16.93030(10)	19.4754(3)	12.7163(4)
α/°	90	90	90.00	90.00
β/°	96.196(3)	98.0580(10)	91.093(2)	90.223(3)

γ/°	90	90	90.00	90.00
Volume/Å^3	12060.6(8)	6759.71(6)	6337.83(19)	5752.2(3)
Z	8	4	4	8
ρ_{calc}mg/mm^3	1.390	1.342	1.242	1.186
m/mm^{-1}	3.152	7.667	2.012	0.696
F(000)	5216.0	2816.0	2520.0	2208.0
Crystal size/mm^3	0.2 × 0.2 × 0.1	0.2 × 0.05 × 0.05	0.3 × 0.07 × 0.04	0.35 × 0.3 × 0.25
2Θ range for data collection	7.132 to 147.97°	6.258 to 147.264°	6.44 to 147.18°	6.4 to 52°
Index ranges	-20 ≤ h ≤ 14, -22 ≤ k	-24 ≤ h ≤ 24, -25 ≤ k	-17 ≤ h ≤ 16, -25 ≤ k ≤ 28, -22 ≤ l ≤ 24	-12 ≤ h ≤ 15, -44 ≤ k ≤
Reflections collected	43761	88776	27288	27792
Independent reflections	23312 [R_{int} = 0.0292]	13479 [R_{int} = 0.0472]	12211[R(int) = 0.0367]	11247[R(int) = 0.0275]
Data/restraints/parameters	23312/0/1315	13479/0/703	12211/23/712	11247/0/639
Goodness-of-fit on F^2	1.031	1.037	1.017	1.159
R_1 ,wR_2 [I>=2σ (I)]	0.0409, 0.0985	0.0277, 0.0717	0.0366, 0.0925	0.0627, 0.1742
R_1 ,wR_2 [all data]	0.0495, 0.1040	0.0302, 0.0735	0.0465, 0.0995	0.0696, 0.1771
Largest diff. peak/ hole / e Å^{-3}	2.76/-0.71	2.47/-0.75	0.36/-0.44	0.63/-0.42
CCDC-	995936	995934	995937	995939

	1-THF
Empirical formula	$C_{36}H_{49}N_2F_6PNiO$
Formula weight	729.45
Temperature/K	123.0(2)
Crystal system	monoclinic
Space group	*Cc*
a/Å	12.7889(2)
b/Å	16.8666(3)
c/Å	16.4852(3)
α/°	90.00
β/°	94.4860(10)
γ/°	90.00
Volume/Å^3	3545.05(11)
Z	4
ρ_{calc}mg/mm^3	1.367
m/mm^{-1}	1.754
F(000)	1536.0
Crystal size/mm^3	0.1974 × 0.0705 × 0.0462
2Θ range for data collection	8.7 to 147.32°
Index ranges	-15 ≤ h ≤ 15, -20 ≤ k ≤ 20, -20 ≤ l ≤ 20
Reflections collected	20803
Independent reflections	6714 [R(int) = 0.0307]
Data/restraints/parameters	6714/2/424
Goodness-of-fit on F^2	1.059
R_1 ,wR_2 [I>=2σ (I)]	0.0258, 0.0661
R_1 ,wR_2 [all data]	0.0268, 0.0671
Largest diff. peak/hole / e Å^{-3}	0.23/-0.26
Flack parameter	-0.007(13)
CCDC-	999501

(S3) EPR spectroscopy

Experimental X-band EPR spectra were recorded on a Bruker EMX spectrometer (Bruker BioSpin Rheinstetten) equipped with a He temperature control cryostat system (Oxford Instruments). Simulations of the EPR spectra were performed by iteration of the anisotropic g-values and line widths using the EPR simulation program W95EPR developed by Prof. Dr. Frank Neese.

Calculation of the EPR properties with DFT

The gas phase geometry of **1** (using the X-ray crystal structure geometry of [CpNi(IDipp)] (**1**) as a starting point) was optimized with the Turbomole program package[10] coupled to the PQS Baker optimizer[11] via the BOpt package[12] at the ri-DFT[13]/BP86[14] level. We used Grimme's D3 dispersion corrections (disp3)[15] and the def2-TZVP basis set[16] for all atoms. The minimum (no imaginary frequencies) was characterized by calculating the Hessian matrix. The Cartesian coordinates of the optimized geometries are supplied in .xyz format.

EPR parameters[17] were calculated with both the ORCA[18] and the ADF[19] program systems, using the coordinates from the structures optimized in Turbomole as input. In the Orca calculations we used the b3-lyp[20] functional and def2-TZVP basis set. In the ADF calculations we used the BP86 functional with the ZORA/TZP basis sets supplied with the program (all electron, core double zeta, valence triple zeta polarized basis set on all atoms). The EPR g-tensors in ADF were obtained from restricted SPINORBIT ZORA calculations.

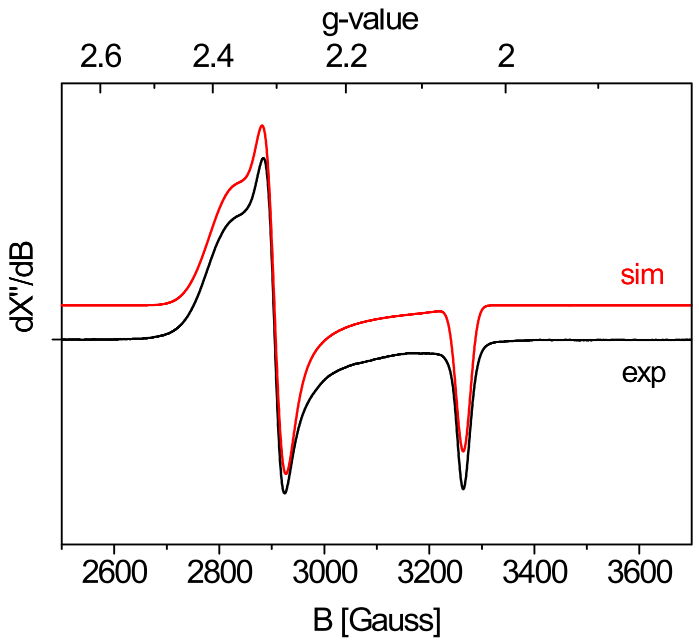

Figure S14. Experimental and simulated X-band EPR spectrum of [CpNi(IDipp)] (**1**) in frozen THF recorded at 20 K (~0.1 M [(nBu$_4$N](PF$_6$) was added to obtain a better glass). Frequency = 9.364601GHz, microwave power = 0.0633 mW, T = 20 K, modulation amplitude = 4 Gauss.

Table 2. Experimental [(a)] and DFT calculated [(b)] EPR parameters of [CpNi(IDipp)] (**1**).

	g_{11} (W) (d)	g_{22} (W) (d)	g_{33} (W) (d)
Exp (a)	2.377 (50)	2.306 (19)	2.050 (16)
DFT (b)	2.220	2.187	2.078
DFT (c)	2.559	2.007	1.930

(a) Obtained by simulation of the experimental spectrum.
(b) Orca, b3-lyp, def2-TZVP.
(c) ADF, BP86, TZ2P.
(d) g-tensor (line width W in MHz).

Cartesian coordinates of [CpNi(IDipp)] (**1**) optimized with Turbomole at the ri-DFT-D3, BP86, def2-TZVP level

76
Energy = -2862.8786196500

C	8.1629980	1.8209051	4.6447538
C	9.4973894	0.0212958	5.1707102
H	10.1099830	-0.6002987	5.8113760
C	9.1343029	-0.1130336	3.8675043
H	9.3642247	-0.8784003	3.1371932
C	7.3365598	5.3005980	3.7258491
H	8.2387069	5.7405040	3.3131112
C	6.4685895	4.3765785	3.0641519
H	6.6044554	3.9743870	2.0638249
C	5.3882004	4.0555039	3.9540119
H	4.5610708	3.3895469	3.7358988
C	5.6113284	4.7414495	5.1767856
H	4.9818432	4.7025377	6.0608740
C	6.8252631	5.5046401	5.0389918
H	7.2678613	6.1345745	5.8059834
C	7.6978182	1.1984684	2.2877897
C	6.3180207	0.9346225	2.1522657
C	5.7445746	1.1771714	0.8980352
H	4.6821830	0.9916141	0.7450134
C	6.5083506	1.6650986	-0.1625419
H	6.0365130	1.8500375	-1.1289474
C	7.8661946	1.9268901	0.0065625
H	8.4445634	2.3209255	-0.8287281
C	8.4921836	1.7003397	1.2394176
C	8.9476263	1.6899533	6.9704014
C	7.9486273	1.2702701	7.8709303
C	7.9921183	1.7946813	9.1687735
H	7.2326750	1.4983185	9.8936381
C	8.9842319	2.7014534	9.5425988
H	8.9986957	3.1008897	10.5579926
C	9.9516316	3.1076294	8.6244045
H	10.7114847	3.8303387	8.9255131
C	9.9539957	2.6112774	7.3140776
C	5.4927007	0.4418667	3.3350095
H	5.7910541	1.0699106	4.1923568
C	5.8007847	-1.0266277	3.6859937
H	5.5364955	-1.6888784	2.8475052
H	5.2110015	-1.3361107	4.5621934
H	6.8594026	-1.1838457	3.9260870
C	3.9810066	0.6146554	3.1491270
H	3.7138295	1.6363655	2.8477822
H	3.4675689	0.3980569	4.0965647
H	3.5791485	-0.0780741	2.3932376
C	9.9540500	2.0615034	1.4704897
H	10.3643031	1.3477306	2.2019128
C	10.8202571	1.9632513	0.2078845
H	10.7165572	0.9851507	-0.2837210
H	11.8783462	2.1049697	0.4703283
H	10.5632822	2.7423790	-0.5247611
C	10.0541406	3.4642993	2.1011299
H	9.6584137	4.2216088	1.4073444
H	11.1029627	3.7147510	2.3208862
H	9.4729245	3.5280977	3.0320584
C	6.8265084	0.3389402	7.4364950
H	7.1016657	-0.0893389	6.4612634
C	5.5264428	1.1364781	7.2285002
H	5.1810119	1.5786384	8.1754594
H	4.7299912	0.4802431	6.8451856
H	5.6869623	1.9510777	6.5037264
C	6.6208250	-0.8312794	8.4097979
H	7.5524534	-1.3947325	8.5615438
H	5.8609479	-1.5219133	8.0158860
H	6.2705380	-0.4857584	9.3933896
C	10.9724826	3.0965203	6.2945276
H	10.8565724	2.4839123	5.3889429
C	10.6772940	4.5529280	5.8953495
H	9.6552325	4.6391180	5.4939633
H	11.3828039	4.8904225	5.1217005
H	10.7693500	5.2258548	6.7613809
C	12.4166999	2.9273456	6.7917003
H	12.6193462	3.5597040	7.6685702
H	13.1266315	3.2190015	6.0041386
H	12.6242346	1.8849959	7.0735174
N	8.3191025	0.9773495	3.5620277
N	8.9000276	1.1909485	5.6276879
Ni	7.2693903	3.4297180	4.8286251

(S4) Electrochemical measurements

Conventional cyclic voltammetry (CV) was performed in a pre-dried air-tight single-compartment cell connected to a Metrohm Autolab PGSTAT302N potentiostat. The cell was equipped with a Pt microdisc (0.14 mm^2) working electrode carefully polished with a 25-µm diamond paste, a Pt coil auxiliary electrode and an Ag coil pseudoreference electrode. The solutions of the studied complexes were prepared under an atmosphere of dry argon in THF freshly distilled from Na/benzophenone. The supporting electrolyte, tetrabutylammonium hexafluorophosphate (TBAH, 10^{-1} mol dm^{-3}) was recrystallized twice from absolute ethanol and dried overnight *in vacuo* at 80 ºC. All redox potentials are reported against the ferrocene/ferrocenium (Fc/Fc$^+$) redox couple used as an internal standard; v = 100 mV s^{-1}.

Controlled-potential electrolyses within the OTTLE cell[21] were carried out using a PA4 potentiostat (Laboratory Devices, Polná, Czech Republic). The concentrations of the dinuclear complexes and TBAH used in these measurements were ca. 5×10^{-4} and 3×10^{-1} mol dm^{-3}, respectively. The UV/Vis spectra were obtained using the Scinco S3100 diode array spectrophotometer. The different redox steps were localized with the aid of the contemporarily recorded thin-layer cyclic voltammograms.

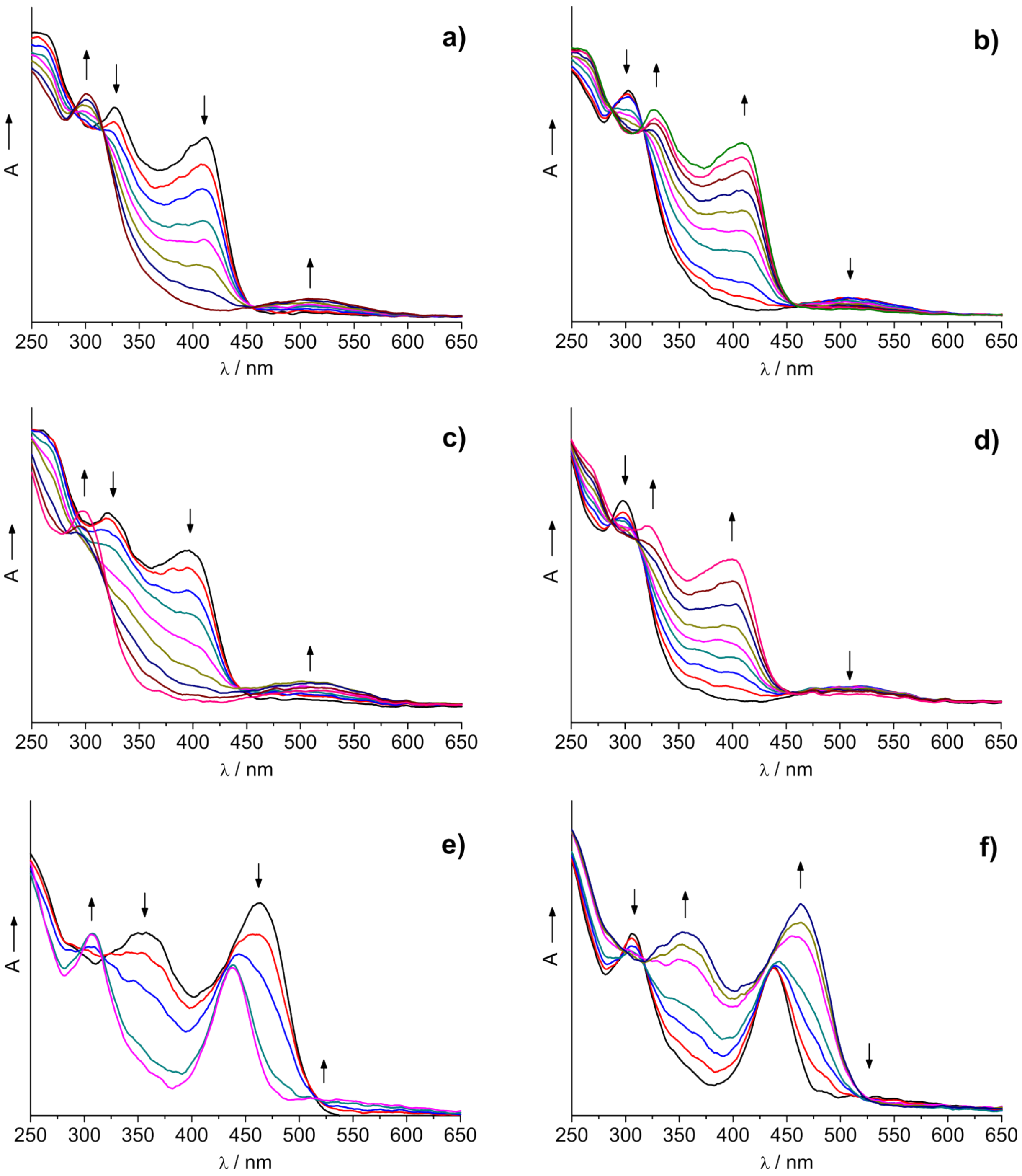

Figure S15: Spectroelectrochemical analysis of compounds **1**–**3**: a) Anodic step $\mathbf{1}\rightarrow\mathbf{1}^+$ monitored in the UV/Vis region; b) reverse cathodic step $\mathbf{1}^+\rightarrow\mathbf{1}$; c) anodic step $\mathbf{2}\rightarrow\mathbf{2}^+$; d) reverse cathodic step $\mathbf{2}^+\rightarrow\mathbf{2}$; e) anodic step $\mathbf{3}\rightarrow\mathbf{3}^+$; f) reverse cathodic step $\mathbf{3}^+\rightarrow\mathbf{3}$. Note the intense absorption band of $\mathbf{3}^+$ at 435 nm, which is absent in the UV/Vis spectra of the Cp-complexes $\mathbf{1}^+$ and $\mathbf{2}^+$.

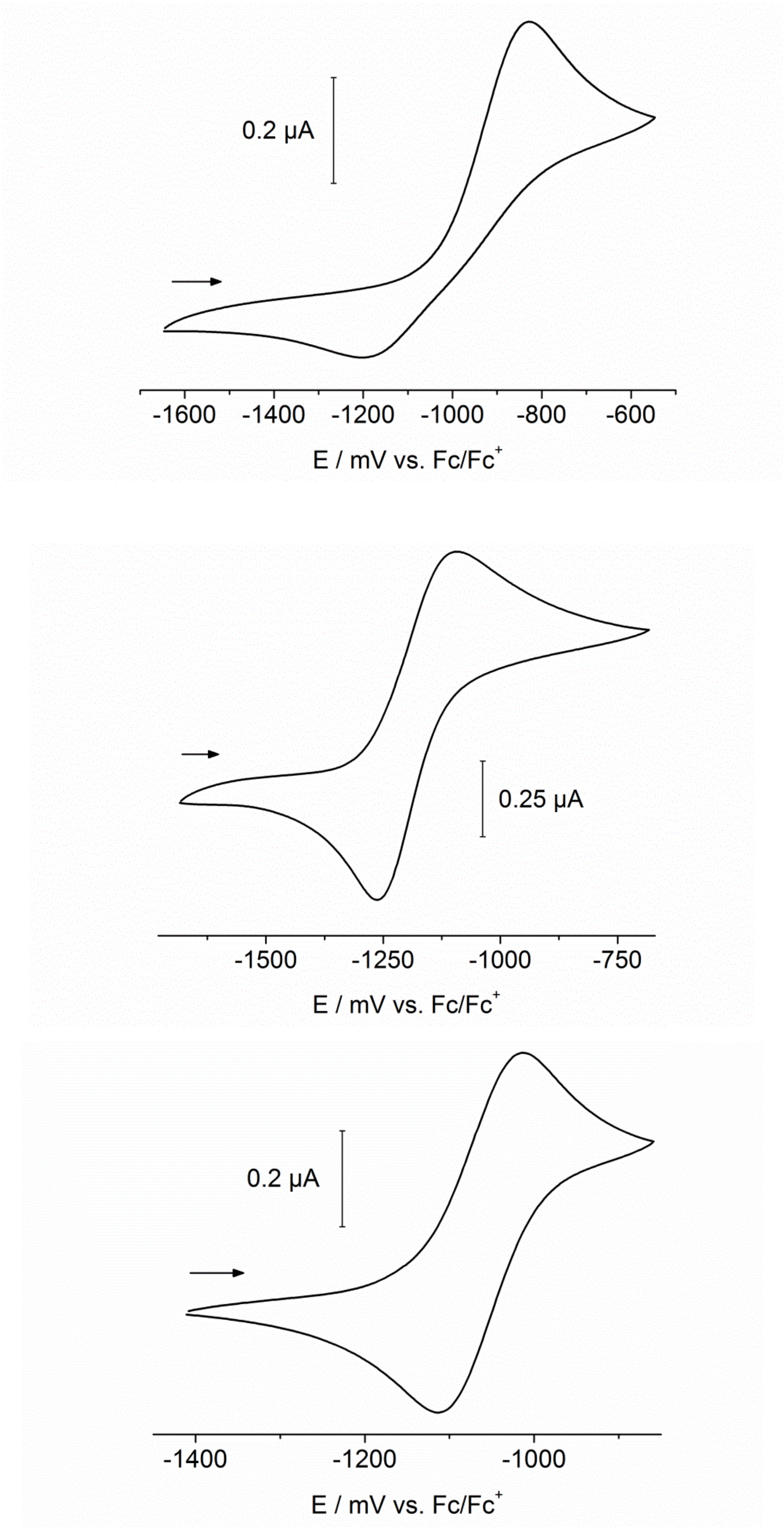

Figure S16: Cyclic voltammograms of compounds **1** (top), **2** (centre), **3** (bottom). Conditions: see above.

References:

1. D. F. Evans, *J. Chem. Soc. Resumed*, 1959, 2003–2005.
2. G. J. P. Britovsek, V. C. Gibson, S. K. Spitzmesser, K. P. Tellmann, A. J. P. White, D. J. Williams, *J. Chem. Soc. Dalton Trans.*, 2002, 1159–1171.
3. S. P. Nolan, 2006, *US Patent:* 7109348.
4. a) R. A. Kelly, N. M. Scott, S. Díez-González, E. D. Stevens, S. P. Nolan, *Organometallics*, 2005, **24**, 3442–3447; b) O. R. Luca, B. A. Thompson, M. K. Takase, R. H. Crabtree, *J. Organomet. Chem.*, 2013, **730**, 79–80.
5. V. Ritleng, C. Barth, E. Brenner, S. Milosevic, M. J. Chetcuti, *Organometallics*, 2008, **27**, 4223–4228.
6. a) *SCALE3ABS*, *CrysAlis*^{Pro}, Aglient Technologies Inc., Oxford, GB, 2012; b) G. M. Sheldrick, *SADABS*, Bruker AXS, Madison, USA, 2007.
7. R. C. Clark, J. S. Reid, *Acta Crystallogr. A*, 1995, **51**, 887–897.
8. G. M. Sheldrick, *Acta Crystallogr. A*, 2007, **64**, 112–122.
9. A. Altomare, M. C. Burla, M. Camalli, G. L. Cascarano, C. Giacovazzo, A. Guagliardi, A. G. Moliterni, G. Polidori, R. Spagna, *J. Appl. Crystallogr.*, 1999, **32**, 115–119.

0. R. Ahlrichs, Turbomole Version 6.5, Theoretical Chemistry Group, University of Karlsruhe.

11. PQS version 2.4, 2001, Parallel Quantum Solutions, Fayettevile, Arkansas (USA); the Baker optimizer is available separately from PQS upon request: I. Baker, *J. Comput. Chem.* 1986, **7**, 385–395.

2. P. H. M. Budzelaar, *J. Comput. Chem.* 2007, **28**, 2226–2236.

3. M. Sierka, A. Hogekamp, R. Ahlrichs, *J. Chem. Phys.* 2003, **118**, 9136.

4. (a) A. D. Becke, *Phys. Rev. A*, 1988**, 38**, 3098. (b) J. P. Perdew, *Phys. Rev. B*, 1986, **33**, 8822.

5. S. Grimme, J. Antony, S. Ehrlich, H. J. Krieg, *J. Chem. Phys.*, 2010, **132**, 154104.

6. a) F. Weigend, R. Ahlrichs, *Phys. Chem. Chem. Phys.* 2005, **7**, 3297–3305; b) F. Weigend, M. Häser, H. Patzelt, R. Ahlrichs, *Chem. Phys. Lett.* 1998, **294**, 143–152.

7. Lead reference for calculation of g-tensor (Zeeman interactions) parameters: E. van Lenthe, A. van der Avoird, P. E. S Wormer, *J. Chem. Phys.* 1997, **107**, 2488. Lead reference for calculation of A-tensor (Nuclear magnetic dipole hyperfine interactions) parameters: E. van Lenthe, A. van der Avoird, P. E. S. Wormer, *J. Chem. Phys.* 1998, **108**, 4783.

8. F. Neese, ORCA – an ab initio, Density Functional and Semiempirical program package, Version 2.9. Max-Planck-Insitut für Bioanorganische Chemie, Mülheim and der Ruhr, 2009

9. ADF2012 a) E. J. Baerends, D. E. Ellis, P. Ros, *Chem. Phys.*, 1973, **2**, 41. b) L. Versluis, T. Ziegler, *J. Chem. Phys.*, 1988, **88**, 322. c) G. te Velde, E. J. Baerends, *J. Comput. Phys.*, 1992, **99**, 84. d) C. Fonseca Guerra, J. G. Snijders, G. te Velde, E. J. Baerends, *Theor. Chem. Acc.*, 1998, **99**, 391.

20. a) C. Lee, W. Yang, R. G. Parr, *Phys. Rev. B*, 1988, **37**, 785–789; b) A. D. Becke, *J. Chem. Phys.*, 1993, **98**, 1372–1377; c) A. D. Becke, *J. Chem. Phys.*, 1993, **98**, 5648–5652; d) Calculations were performed using the Turbomole functional "b3-lyp", which is not completely identical to the Gaussian "B3LYP" functional.
21. M. Krejčík, M. Daněk, F. Hartl, *J. Electroanal. Chem.* 1991, **317**, 179.